On global monsoons – further results

By M. SANKAR-RAO,[1] *Goddard Institute for Space Studies, New York*

(Manuscript received April 4, 1970; revised version September 8, 1970)

ABSTRACT

In continuation of a previous study, the global monsoonal response of the atmosphere is computed within the framework of a quasi-geostrophic model. The input parameters are the ground temperature, mountain heights and the zonal mean state at 45° N. A parameterized heating function given in the earlier work is utilized. Lateral friction, conduction and mountains are also taken into account. It is found that the computed global monsoons are closer in phase and magnitude to the observed ones. The energetics and the other interesting results are discussed.

Introduction

In a previous paper by Sankar-Rao & Saltzman (1969), hereafter to be referred to as Paper I, a steady state theory of global monsoons was presented within the framework of a drastically simplified linear model. A heating function comprising of two parts was proposed. Computations of the atmospheric response only for the first part of the heating function were presented. The main result was that the computed global monsoonal systems, though of right magnitude, were displaced towards the east of the observed climatic systems. It was conjectured in the same paper that the phase discrepancy will be remedied to some degree by including the second part of the heating function. The main purpose of the present paper is to give the results obtained by including the complete heating function, mountains, the lateral friction and the lateral conduction. The notation is the same as in Paper I. The following values are given the respective parameters:

A_1 = 100 ergs g^{-1} sec^{-1} deg^{-1}.

A_2 = 1.5×10^7 ergs g^{-1} deg^{-1}. (For a surface wind velocity of 100 cm sec^{-1} and for a surface temperature gradient of 8×10^{-8} deg cm^{-1}, this value of A_2 gives a boundary heat flux of the order of 0.3×10^6 ergs cm^{-2} sec^{-1}.)

$K_{HM} = K_{HT} = 10^9$ cm^2 sec^{-1}.

[1] NRC-NAS Resident Research Associate.

The mountain amplitudes were taken from a previous paper by Sankar-Rao (1965). All other parametes are the same as in Paper I. In addition to the usual computed maps, the energy conversion terms at 45° N will also be discussed in this paper.

Discussion of the results

Figs. 1 to 4 give the winter results (Experiment 1), while the Figs. 5 to 8 give the summer results (Experiment 2). Because the mean zonal parameters at 45° N were utilized in these computations, the results over the Southern Hemisphere cannot be discussed. As far as the Northern Hemispheric results are concerned, it can be seen that the positions as well as the magnitudes of the global monsoonal pressure systems for both the seasons show a closer resemblance to the observed climatic maps, both at the surefac and at the 300-mb level. Strong heating off the east coast in winter can be noticed in Fig. 4. Strong heating towards the leeward side of the Himalayas may be due to the limitations of this linear model in the incorporation of the mountain effect. In summer strong heating over the desert regions can be noticed in Fig. 8. From Fig. 7 one can notice that over these desert regions, descending motion prevails, in spite of general heating. This may be a partial explanation of the desert regions over the globe. The Tables 1 and 2 give the energy conversion terms for winter and summer. The meaning of each term is the following:

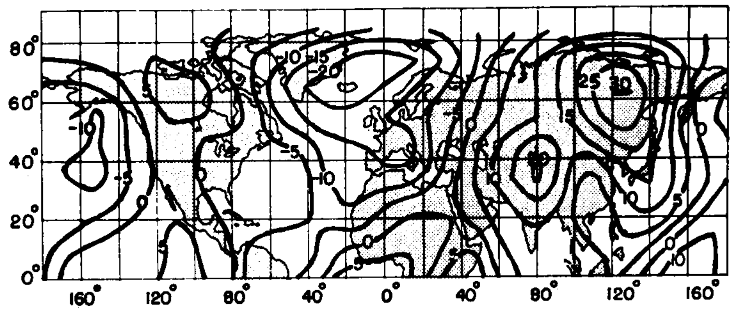

Fig. 1. Geopotential of 900-mb level in 10^{-3} cm^2 sec^{-1}, which corresponds approximately to millibars at sea level. Experiment 1, 15th degree map.

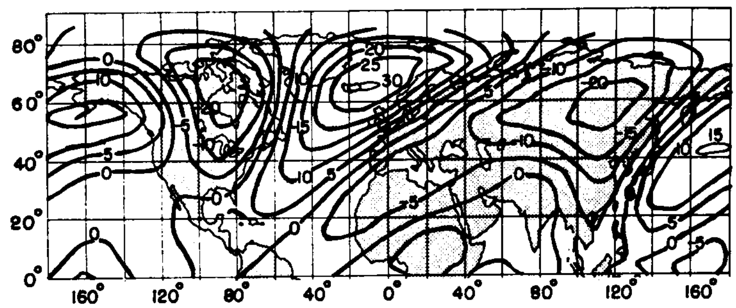

Fig. 2. Same as Fig. 1, but for 300-mb level.

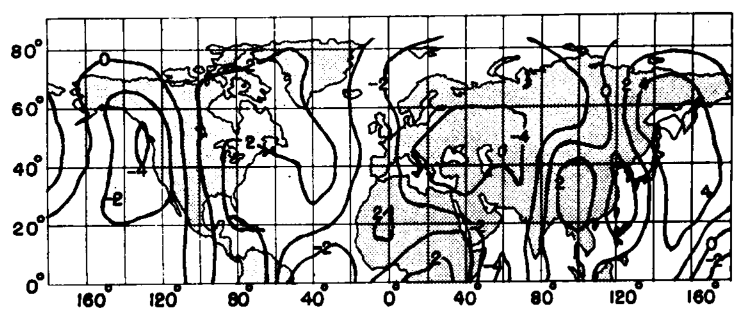

Fig. 3. The rate of change of pressure, ω_*, in 10^{-1} g cm^{-1} sec^{-3} 300-mb level. Experiment 1, 15th degree map.

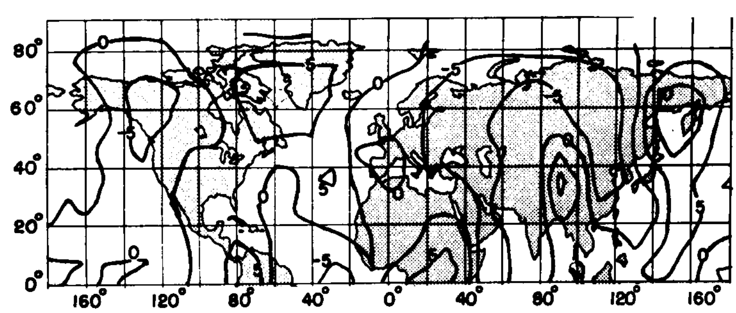

Fig. 4. Vertically integrated heating, $\dot{Q}_*$, in 10^5 ergs cm^{-2} sec^{-1}. Experiment 1, 15th degree map.

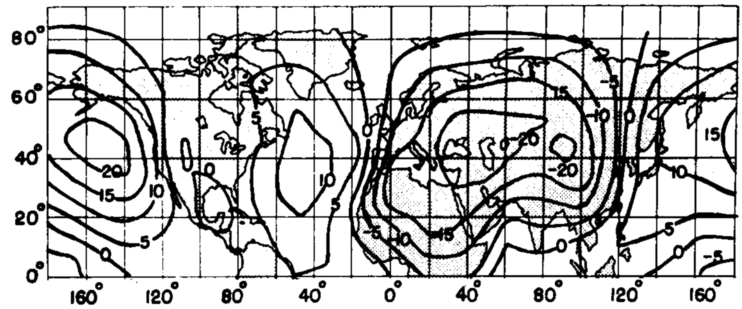

Fig. 5. Same as Fig. 1, but for Experiment 2.

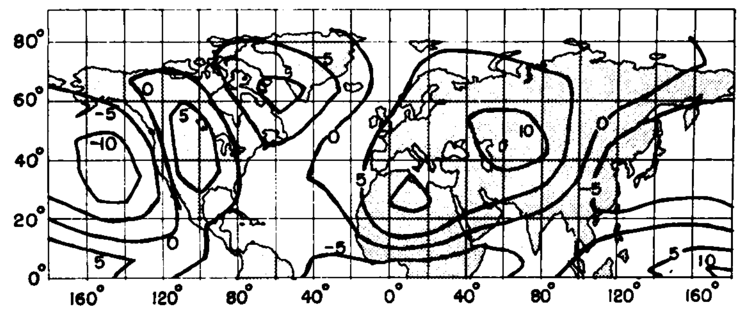

Fig. 6. Same as Fig. 2, but for Experiment 2.

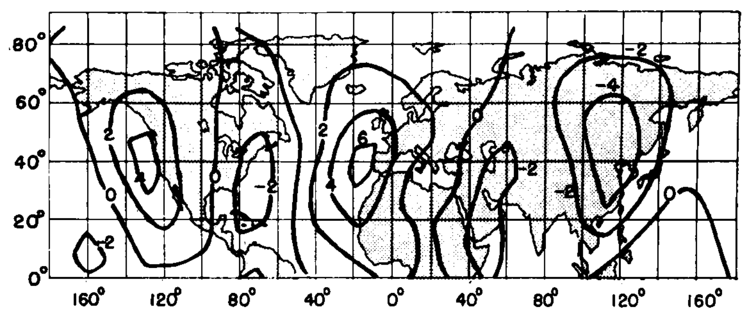

Fig. 7. Same as Fig. 3, but for Experiment 2.

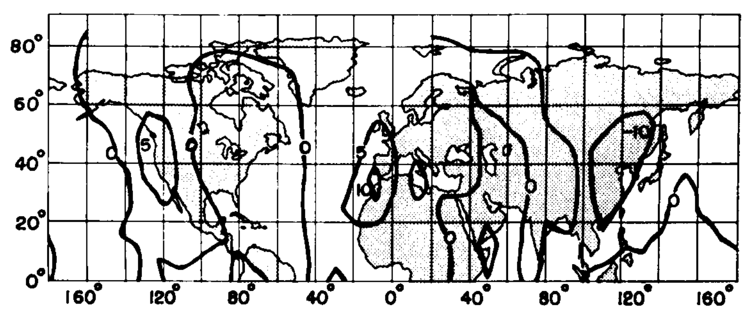

Fig. 8. Same as Fig. 4, but for Experiment 2.

Table 1. *Energy conversion terms (winter) expt. 1*

m	n	$I(Q_s, A_s)$	$I(A_z, A_s)$	$I(A_s, K_s)$	$I(A_s, F_T)$	$I(h_s, P_s)$	$I(K_s, F_\delta)$	$I(K_s, F_H)$
1	1	31.10	−12.43	18.05	0.63	−12.95	4.99	0.02
1	2	335.52	145.36	178.26	11.91	−41.48	134.48	0.78
2	2	−15.49	20.65	3.52	1.68	21.65	17.86	0.11
1	3	117.84	−65.90	46.96	4.99	0.12	46.30	0.52
2	3	612.99	−354.84	241.95	16.20	−94.65	144.53	1.76
3	3	3.60	−0.11	2.76	0.72	8.86	11.50	0.07
1	4	0.53	−0.31	−0.16	0.05	0.31	0.45	0.01
2	4	555.96	−380.92	153.21	22.35	−21.46	127.42	3.66
3	4	560.00	−405.59	149.46	4.97	−88.00	60.25	1.01
4	4	22.36	−14.99	6.75	0.62	6.61	13.23	0.10
1	5	67.37	−53.39	8.49	5.49	0.91	7.29	2.06
2	5	71.73	−58.37	9.22	4.13	2.17	10.16	1.17
3	5	962.13	−838.24	108.64	15.26	−10.46	92.90	5.02
4	5	962.40	−846.04	107.33	9.04	−0.42	103.74	2.97
5	5	45.79	−40.45	5.04	0.30	−1.05	3.86	0.11
1	6	−58.58	81.93	15.31	8.04	25.09	37.41	2.94
2	6	−30.41	38.80	6.32	2.07	−0.50	4.78	1.00
3	6	−74.29	88.44	12.41	1.74	1.95	12.32	2.03
4	6	146.78	−167.03	−20.81	−0.57	105.78	81.92	3.03
5	6	52.83	−59.90	−7.37	0.31	17.41	9.60	0.44
6	6	6.25	−7.08	−0.87	0.04	1.67	0.76	0.04
1	7	−0.60	3.92	2.28	1.03	−0.65	1.05	0.59
2	7	−17.67	39.82	17.98	4.18	11.60	28.34	1.22
3	7	−0.03	0.06	0.02	0.00	0.01	0.03	0.00
4	7	−9.25	15.56	6.10	0.21	1.71	7.62	0.19
5	7	−23.69	−42.80	17.78	1.33	−14.87	1.91	0.99
6	7	−2.78	5.44	2.30	0.36	2.54	4.75	0.08
7	7	0.34	−0.49	−0.17	0.02	0.20	0.02	0.01
1	8	−0.04	0.17	0.11	0.01	0.17	0.27	0.02
2	8	−0.27	0.91	0.60	0.04	1.55	2.09	0.06
3	8	−4.93	16.56	11.21	0.43	2.97	13.77	0.41
4	8	−1.44	5.22	3.53	0.24	3.26	6.65	0.13
5	8	−7.41	29.94	21.12	1.41	11.58	9.03	0.51
6	8	0.38	−1.17	−0.79	0.01	1.92	1.06	0.07
7	8	2.51	−6.36	−4.13	0.28	6.38	2.16	0.09
8	8	0.022	−0.044	−0.027	0.004	0.040	0.012	0.002

$I(Q_s, A_s)$ = Production of stationary wave available potential energy.

$I(A_z, A_s)$ = Conversion of zonal available potential energy to the stationary wave available potential energy.

$I(A_s, K_s)$ = Conversion of stationary wave available potential energy to stationary wave kinetic energy.

$I(A_s, F_T)$ = Destruction of stationary wave available potential energy by lateral conduction.

$I(h_s, P_s)$ = Production of stationary wave kinetic energy by the mountain effect.

$I(K_s, F_\delta)$ = Destruction of the stationary wave kinetic energy by surface friction.

$I(K_s, F_M)$ = Destruction of the stationary wave kinetic energy by lateral friction.

In the tables, the units of these terms are in 10^3 g sec^{-3}. The equations for the energy conversions in this model take the form

$$I(A_s, K_s) + I(h_s, P_s) - I(K_s, F_\delta) - I(K_s, F_H) = 0$$

$$I(A_z, A_s) - I(A_s, K_s) + I(Q_s, A_s) - I(A_s, F_T) = 0$$

The formulas for these terms can be derived quite easily and will not be given here (e.g., Murakami, 1967).

From Table 1 the following points can be inferred for winter:

1. The lower wave numbers up to and including $(m, n) = (6, 6)$ contribute most to the energy of the stationary systems. Other wave

Table 2. *Energy conversion terms (summer) expt. 2*

m	n	$I(Q_s, A_s)$	$I(A_z, A_s)$	$I(A_s, K_s)$	$I(As, F_T)$	$I(h_s, P_s)$	$I(K_s, F_\delta)$	$I(K_s, F_H)$
1	1	7.44	1.54	7.72	1.26	9.73	17.43	0.24
1	2	728.89	−283.48	416.14	29.28	−56.65	357.97	1.46
2	2	59.92	−25.63	33.00	1.28	−17.20	15.73	0.07
1	3	66.99	−33.12	31.57	2.30	−5.25	26.11	0.21
2	3	173.38	−78.47	88.87	6.04	−2.90	85.39	0.56
3	3	14.05	−5.95	7.47	0.63	0.93	8.34	0.06
1	4	0.09	−0.05	0.03	0.01	−0.01	0.01	0.00
2	4	382.97	−216.84	154.73	11.40	−26.90	126.21	1.60
3	4	22.37	−1.60	14.19	6.57	51.95	65.31	0.85
4	4	30.51	−17.86	12.22	0.44	−7.19	4.96	0.06
1	5	236.27	−153.73	66.02	16.52	−0.88	60.65	4.54
2	5	13.89	−9.19	4.10	0.60	−0.53	3.43	0.13
3	5	−12.68	10.05	3.38	0.75	7.28	3.75	0.16
4	5	132.75	−83.36	43.57	5.83	23.63	66.17	1.01
5	5	2.40	−1.44	0.84	0.13	0.89	1.70	0.02
1	6	6.10	−0.55	2.00	3.55	4.52	5.32	1.21
2	6	2.13	−1.66	0.36	0.11	0.39	0.72	0.04
3	6	11.51	−9.21	1.87	0.43	−0.43	1.25	0.19
4	6	169.60	−138.18	27.68	3.74	2.03	28.39	1.31
5	6	5.34	−4.46	0.85	0.03	0.54	1.34	0.04
6	6	0.09	−0.07	0.01	0.00	0.05	0.06	0.00
1	7	1.08	−0.73	0.12	0.23	0.19	0.13	0.19
2	7	7.35	−7.07	0.18	0.46	4.34	3.96	0.20
3	7	0.00	−0.00	0.00	0.00	0.00	0.00	0.00
4	7	−3.75	4.68	0.56	0.35	0.16	0.40	0.34
5	7	−33.91	38.18	3.35	0.92	10.36	13.32	0.39
6	7	−0.23	0.42	0.10	0.10	2.21	2.00	0.30
7	7	−0.32	0.36	0.03	0.00	0.31	0.33	0.00
1	8	0.012	0.017	0.015	0.014	0.026	0.035	0.006
2	8	−4.34	8.26	3.22	0.70	0.42	0.31	0.52
3	8	−1.60	2.59	0.91	0.08	0.31	1.05	0.17
4	8	−0.58	1.00	0.37	0.05	−0.09	0.24	0.03
5	8	−11.29	19.49	7.12	1.08	0.41	7.11	0.43
6	8	−8.07	12.06	3.90	0.09	2.52	5.95	0.48
7	8	−0.34	1.10	0.54	0.21	0.81	1.28	0.07
8	8	0.06	−0.08	−0.02	0.00	0.05	0.003	0.00

numbers play an insignificant part. The waves $(m,n) = (3,5)$ and $(4,5)$ produce the maximum avaialable potential energy.

2. Almost all these long waves derive their energy from the stationary heat sources and sinks, but $(m,n) = (2,2)$, $(1,6)$, $(2,6)$ and $(3,6)$ seem to be exceptions to this rule. They derive their energy from the zonal mean motion. This result agrees well with Murakami's (1967) results but seems to contradict the observational results of John A. Brown, Jr (1964), where he finds that in winter the available potential energy is generally destroyed by the long waves. This is a serious discrepancy. However, in view of the simplified nature of the theory presented here and in view of the shortcomings in the observational analysis, one can only hope to resolve this question in the future.

3. The lateral friction and conduction play a very insignificant role in the energetics.

4. For most of the long waves the mountain effect is to destroy the eddy kinetic energy.

From Table 2 the following inferences can be drawn for summer:

1. Again, as in the case of winter, the long waves up to and including $(m, n) = (6,6)$ are most important for the maintenance of the global monsoons.

2. The wave number $(m,n) = (1,2)$ produces the maximum available potential energy. The wave numbers $(3,5)$ and $(4,5)$, which produce maximum eddy available potential energy in winter, play a minor role in summer.

3. The effects of lateral friction, lateral con-

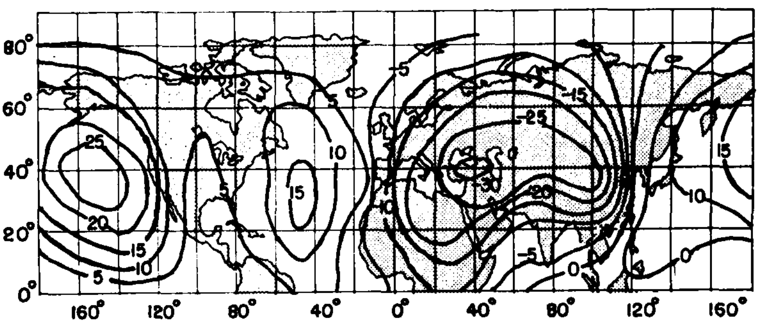

Fig. 9. Same as Fig. 1, but for Experiment 3.

duction and the mountains resemble the winter behavior.

The linear model has obvious limitations. For instance, when the forcing mode is of the same wave number as that of a baroclinically unstable wave, resonance can result in a linear model. Under idealized conditions, the response must be infinite in such a case. But because the

Table 3. *Energy conversion terms (summer) expt. 3*

m	n	$I(Q_s, A_s)$	$I(A_z, A_s)$	$I(A_s, K_s)$	$I(A_s, F_T)$	$I(h_s, P_s)$	$I(K_s, F_\delta)$	$I(K_s, F_H)$
1	1	31.76	−11.1	20.60	0.0	18.70	39.28	0.0
1	2	1192.10	−502.40	689.72	0.0	−100.99	587.97	0.0
2	2	91.56	−38.59	52.98	0.0	−30.65	22.27	0.0
1	3	89.95	−45.15	44.80	0.0	−7.72	37.05	0.0
2	3	219.14	−110.00	109.15	0.0	6.01	115.07	0.0
3	3	18.20	−9.13	9.06	0.0	1.94	11.00	0.0
1	4	0.10	−0.06	−0.04	0.0	−0.03	0.01	0.0
2	4	471.98	−280.41	191.57	0.0	−35.36	156.08	0.0
3	4	−19.74	11.73	8.01	0.0	84.18	76.17	0.0
4	4	43.33	−25.74	17.59	0.0	11.36	6.21	0.0
1	5	238.39	−169.28	69.11	0.0	−1.85	67.21	0.0
2	5	15.61	−11.09	4.52	0.0	−0.87	3.65	0.0
3	5	−27.61	19.61	8.00	0.0	12.07	4.04	0.0
4	5	164.82	−117.04	47.78	0.0	44.41	92.17	0.0
5	5	3.16	−2.24	0.92	0.0	1.67	2.59	0.0
1	6	−5.77	5.04	0.72	0.0	8.33	7.60	0.0
2	6	2.75	−2.40	3.44	0.0	0.82	1.16	0.0
3	6	14.89	−13.02	1.86	0.0	−0.21	1.65	0.0
4	6	274.48	−240.07	34.41	0.0	16.35	50.73	0.0
5	6	12.49	−10.92	1.57	0.0	2.31	3.88	0.0
6	6	0.51	−0.44	0.06	0.0	0.17	0.24	0.0
1	7	0.91	−1.04	0.13	0.0	0.51	0.39	0.0
2	7	11.58	−13.24	1.66	0.0	10.48	8.81	0.0
3	7	0.002	−0.002	0.00	0.0	0.001	0.001	0.0
4	7	−8.36	9.56	−1.20	0.0	0.47	1.67	0.0
5	7	−23.61	26.99	3.39	0.0	29.93	33.32	0.0
6	7	0.42	−0.48	0.06	0.0	6.71	6.65	0.0
7	7	0.53	−0.60	0.08	0.0	0.97	0.89	0.0
1	8	−0.007	0.012	0.005	0.0	0.057	0.061	0.0
2	8	−6.04	10.17	4.13	0.0	0.97	5.10	0.0
3	8	−1.94	3.27	1.33	0.0	0.53	1.85	0.0
4	8	−0.48	0.80	0.33	0.0	−0.02	0.30	0.0
5	8	−4.95	8.33	3.39	0.0	6.71	10.10	0.0
6	8	−7.68	12.94	5.26	0.0	4.18	9.44	0.0
7	8	2.29	−3.85	1.57	0.0	3.86	2.30	0.0
8	8	0.13	−0.22	0.09	0.0	0.15	0.06	0.0

profiles of the zonal mean variables such as K_0, U_0 and $(1/a(\partial T_0/\partial\varphi)$ are obtained from observations and differ significantly from idealized distributions, one can expect subdued type of resonance, which is termed as "quasi-resonance". The inclusion of friction and conduction also limits the resonant amplitudes and helps in producing only "quasi-resonance". However, the question arises whether one can apply linearization assumptions under "quasi-resonant" conditions. Indeed, there are many such limitations for a linear theory presented here. Hence one cannot ask this model any detailed questions. However, the model can at least give a correct indication of what happens if some of the parameters are changed.

So it is felt that it will be of some interest to know what might probably happen if the mean zonal surface wind velocity is increased by 1 msec^{-1}. Because the zonal wind velocity at all other levels is calculated by the thermal wind equation, this is equivalent to an increase of 1 msec^{-1} in the zonal mean wind velocity at all levels. The results of such an experiment for summer monsoon (Experiment 3) are given in Fig. 9. One can notice the general strengthening of the summer monsoon over Asia and a stronger ridge over the Indian Subcontinent in these figures. Table 3 gives the energy conversion results for this experiment. From this table one can infer that the most important wave number $(m,n) = (1,2)$ shows nearly 50% increase in the production of available potential energy. All the other important waves show considerably less percentual increase. Thus it can be concluded that the wave number $(m,n) = (1,2)$ is responsible for the general strengthening of the summer monsoon in this case. One can expect stronger response in this case, because the lateral friction and conduction are not included. Hence, caution does not permit one to conclude from this result that the variations in the general zonal circulation are in general positively related to the strength of the Asian summer monsoon except over the Indian Subcontinent. At least this result suggests one parameter that can be important in the observational studies of such important phenomena as the summer droughts and floods over Asia.

Acknowledgements

The author thanks the National Academy of Sciences for supporting this work. I thank Dr Robert Jastrow for all the facilities given at the Goddard Institute for Space Studies in New York. My thanks are also due to the Department of Aeronautics, Indian Institute of Science, Bangalore, for the kind help in preparing these figures.

REFERENCES

Brown, John A., Jr. 1964. A diagnostic study of tropospheric heating and the generation of available potential energy. *Tellus 16*, 371–388.

Murakami, T. 1967. Vertical transfer of energy due to stationary disturbances induced by topography and diabatic heat sources and sinks. *J. Meteor. Soc. Japan 45*, 205–230.

Sankar-Rao, M. 1965. Continental elevation influence on the stationary harmonics of the atmospheric motion. *Pure and Appl. Geophys. 60*, 141–159.

Sankar-Rao, M. & Saltzman, B. 1969. On a steady state theory of global monsoons. *Tellus 21*, 308–329.

О ГЛОБАЛЬНЫХ МУССОНАХ — ДАЛЬНЕЙШИЕ РЕЗУЛЬТАТЫ

В продолжение предыдущих исследований в рамках квазигеострофической модели вычислена глобальная муссонная переходная функция атмосферы. Входными параметрами являются наземная температура, высота гор и среднее состояние зонального движения для 45° с. ш. Используется параметризованная функция нагревания, данная в предыдущей работе. Боковое трение, проводимость и горы также приняты во внимание. Найдено, что рассчитанные глобальные муссоны близки по фазе и величине к наблюдаемым. Обсуждаются энергетика муссонов и другие интересные результаты.